



Controlling Nitrogen Oxide and Ultraviolet-A irradiance in ventilation duct system using TiO₂ photocatalyst

Yong Woo Song, Seong Eun Kim, Yong Gi Jung, Jae Yun Yoo, Jin Chul Park^{*}

Chung-Ang University, Seoul, 06794, Republic of Korea

ARTICLE INFO

Keywords:

TiO₂ photocatalyst
Ventilation system
Particulate matter
Nitrogen oxides
Reduction test

ABSTRACT

In this study, we verified the application of TiO₂ photocatalysts on ventilation ducts used in buildings and their effects on reducing nitrogen oxide (NO_x), which is a typical particulate matter precursor. The TiO₂ photocatalyst produces a radical dioxide with a strong acid oxidation power through photochemical reactions with ultraviolet-A (UV-A) rays and removes NO_x through oxidation. The removal experiment was conducted by applying TiO₂ photocatalyst coatings inside the duct to comply with the conditions of the ISO 22197-1: 2007. In addition, changes in the NO_x removal were confirmed through changes in the concentration of NO_x and UV-A irradiance inside the duct. At approximately 100 min after switching on the UV-A lamp during the experiment conducted according to ISO 22197-1: 2007, the NO_x concentration decreased to 0.053 ppm (by 94.87%). Moreover, it has been confirmed that the trend of reduction is proportional to the changes in UV-A irradiance and NO_x concentration, that is, an increase in UV-A irradiance has a significant impact on the reduction of NO_x concentration; NO_x reduction increases as a secondary function due to an increase in the UV-A irradiance. Through this study, it is believed that NO_x, a representative precursor material that generates particulate matter, can be removed through a building ventilation system using a TiO₂ photocatalyst.

1. Introduction

The average annual fine particulate matter (PM) (i.e., PM_{2.5}) concentration in South Korea was 24.8 µg/m³ in 2019 according to the annual report of the Organization for Economic Cooperation and Development (OECD), which is the highest average PM_{2.5} level in any OECD country [1]. In Seoul, a daily average concentration of approximately 25 µg/m³ was experienced for 141 days from 2014 to 2016. The number of days showing this concentration exceeded the daily average standard given by the World Health Organization recommendation and has significantly increased in recent years [2]. In particular, the monthly average concentration was the highest (30–32 µg/m³) during winter (December to March) [3].

The indoor space, where most people spend a large fraction of their time performing various activities, poses a high risk of PM exposure, which is introduced from the outside. Indoor PM exposure affects the human body more significantly compared to that of outdoor spaces. This is owing to the limited air circulation [4–6] and has adverse health effects on the cardiovascular and respiratory systems. Because the outside

air used for building ventilation is no longer fresh air, especially with severe outdoor pollution, the outside air that is introduced inside must be purified to dilute various pollutants included in the air [7–9].

The chemical and physical nature of PM in South Korea is mainly attributed to its components from chemical reactions with gaseous precursors, including nitrogen oxides, sulfur oxides, and volatile organic compounds (VOCs) that generate PM in the atmosphere [10,11]. The removal of these precursors is effective in reducing PM concentrations in the atmosphere and indoors.

TiO₂ photocatalysts form OH and O₂-radicals with strong oxidizing power on the surface through photochemical reactions with ultraviolet-A (UV-A) rays (350–380 nm) present in the atmosphere and decompose pollutants. The photocatalytic oxidation mechanism of nitrogen oxides is shown in Equations (1)–(8) [12,13]:



^{*} Corresponding author. School of Architecture and Building Science, Chung-Ang University, Seoul, 06974, Republic of Korea.

E-mail addresses: yongma0930@cau.ac.kr (Y.W. Song), asteria03@naver.com (S.E. Kim), popopop12@naver.com (Y.G. Jung), jyoon6142@naver.com (J.Y. Yoo), jincpark@cau.ac.kr (J.C. Park).

<https://doi.org/10.1016/j.buildenv.2021.107881>

Received 15 March 2021; Received in revised form 6 April 2021; Accepted 7 April 2021

Available online 21 April 2021

0360-1323/© 2021 Elsevier Ltd. All rights reserved.

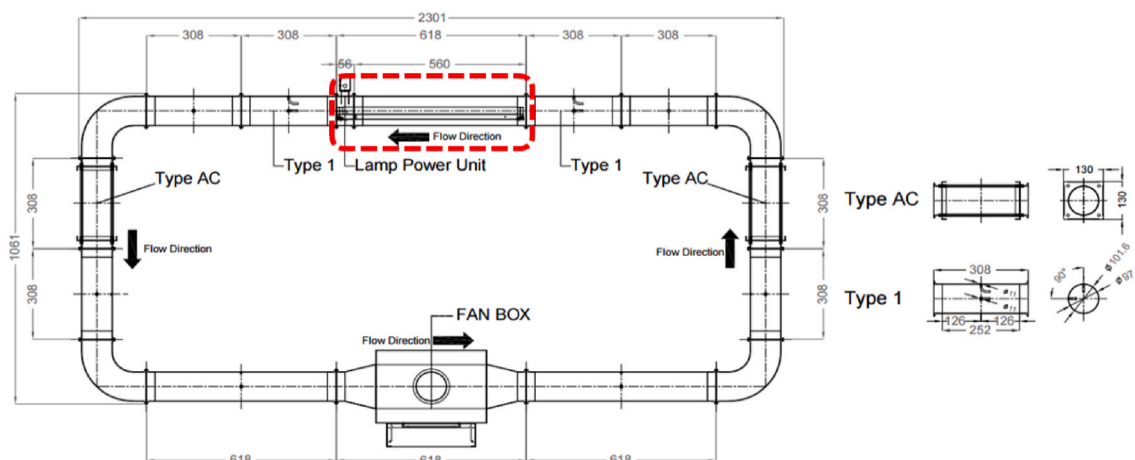


Fig. 1. Design of the TiO₂ photocatalyst ventilation duct system.

Table 1

TiO₂ coating paint composition ratio.

Contained Chemicals	Proportion
Titanium dioxide(anatase)	1.75%
Silicone compound	5.6%
Ethanol	41.6%
Water	51.0%
Other	0.05%

Table 2

Overview of FESEM and EDS mapping equipment.

Classification	Contents
Model	SIGMA 500 (Carl Zeiss)
Detector	SE 2
EDS detector	X-Max ^N 50 (Oxford)
Acceleration voltage	18.0 kV
Working distance	8.5 mm
Magnification	500x to 1,000x
Time-resolution	0.8 nm

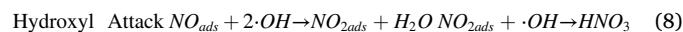


Fig. 2. FESEM and EDS mapping equipment.

Table 3

Results of FESEM and EDS mapping analysis. A (Spectrum before applying TiO₂ coating). B (Spectrum after applying TiO₂ coating).

Element	Before TiO ₂ coating (Wt%)	After TiO ₂ coating (Wt%)	Change value (%)
C	12.84	3.47	−9.37
O	3.04	65.09	+62.05
Al	79.34	10.39	−68.95
Cu	4.79	–	−4.79
Ti	–	21.05	+21.05
Total	100.0	100.0	0



where $h\nu$ is the energy of the UV radiation, $Site^{**}$ is the surface of TiO_2 , and $\cdot OH$ is the hydroxyl radical.

As observed in Equations (1)–(8), when TiO₂ on the material surface absorbs UV energy from sunlight, holes (h⁺) and electrons (e[−]) are generated (Equation (1)). •OH and O₂ • radicals with strong oxidizing powers are generated on the surface of TiO₂ through reactions with H₂O and O₂ in the atmosphere (Equations (2)–(7), electron trapping). This process generates reactive oxygen species [14], and NO_x, a representative precursor, can be decomposed (8).

Representative studies on the application of TiO₂ photocatalysts, studies on the effects of adding TiO₂ photocatalysts to building materials, such as concrete [15,16], mortar [17,18], porous blocks [18], and stone have been conducted. Further, researchers have examined the removal of nitrogen oxides and sulfur oxides generated on roads by applying TiO₂ photocatalyst coatings to asphalt surfaces, which make up most road pavements [19,20]. Previous studies have also examined the PM trend according to the ISO-22197-1 experimental conditions and other conditions using coating agents mixed with TiO₂ photocatalysts.

Luigi Cassar et al. conducted research on the application of TiO_2 photocatalysts to concrete used as a building exterior material. They had applied TiO_2 photocatalysts on external materials used on the Jubilee Church, Rome, and road pavements as a test and found an improvement in antifouling performance and a 30–40% reduction in air pollution [15]. In contrast, Luna et al. applied TiO_2 photocatalyst coatings to the surface of limestone and granite and found that granite is superior to limestone in terms of antifouling performance and soot removal [21]. Furthermore, Lettieri et al. also verified the loss of the antifouling performance in eight months and the NO_x reduction performance by employing TiO_2 photocatalyst coatings to the surface of limestone [22]. Ramirez et al. performed an experiment by applying TiO_2 photocatalyst coatings and particle injection to porous cementitious materials and found that the particle injection method and porous materials have high toluene removal efficiency [18]. In addition, Song et al. examined the trend according to the ISO-22197-1 conditions and other conditions

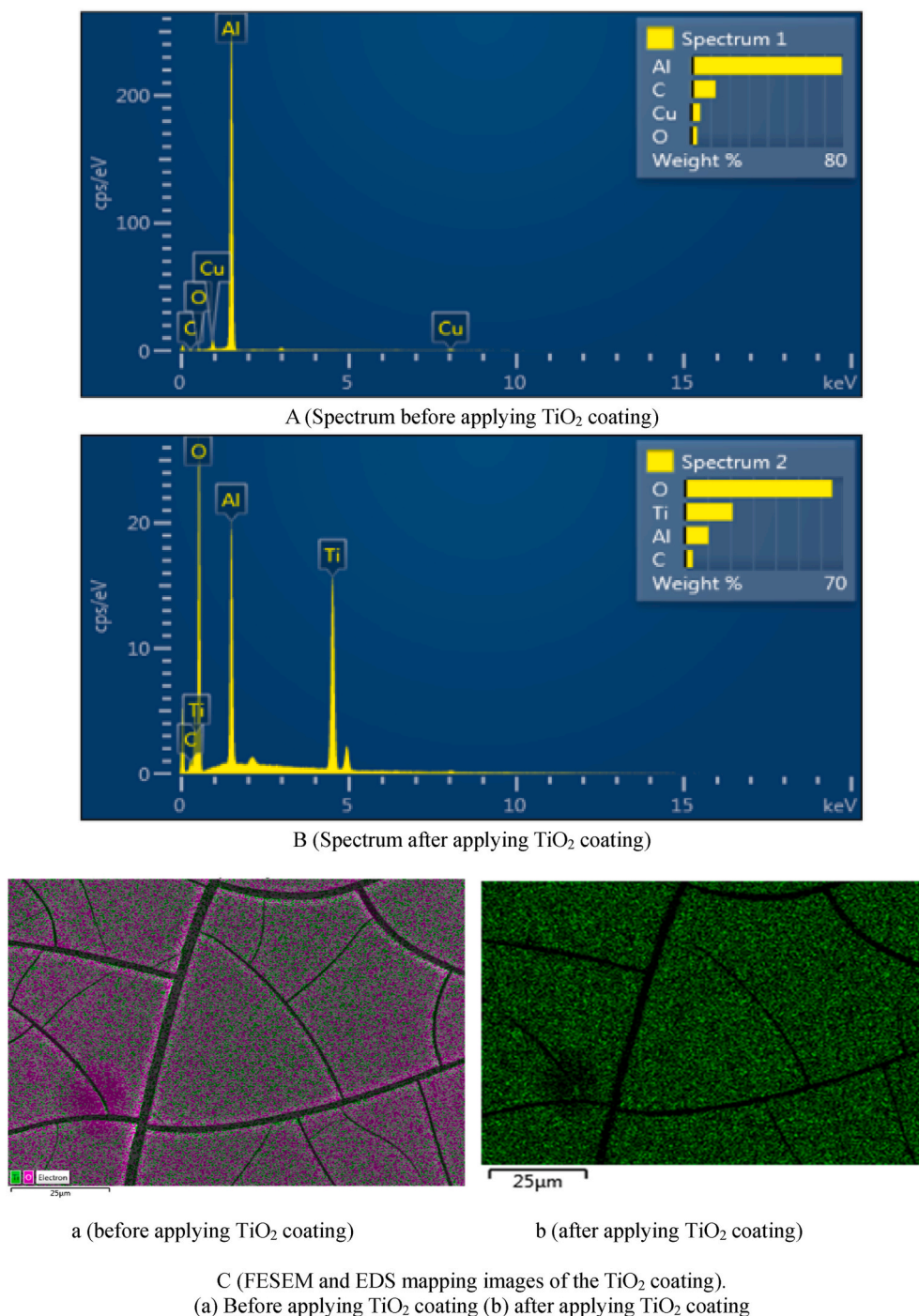


Fig. 3. Results of FESEM and EDS mapping analysis before and after TiO₂ coating application.

(irradiance and NO_x concentration) using coating agents mixed with TiO₂ photocatalysts [23].

In previous studies on the application of TiO₂ photocatalysts to air purifiers, Le et al. and Zhao et al. performed experiments on air purification and sterilization in hospitals and buildings by combining TiO₂ photocatalytic filters with nano-silver-coated filters [24]. They found that VOCs and bacteria were removed, 80% of acetone was removed within 100 min, and 43% of benzene was removed within 150 min. It was also found that 68–99% of bacteria and fungi were killed after they passed through the equipment [25].

As for additional studies on the combination of air purifiers and TiO₂ photocatalysts, Kim et al. applied a TiO₂ photocatalyst filter to an air

purifier and found that the total volatile organic compounds generated during smoking were reduced by approximately 96% [26]. In addition, Yu et al. examined the VOC removal efficiency of a TiO₂ photocatalytic filter according to the HVAC system humidity conditions [27]. Ao and Lee examined the NO and NO₂ removal performance of an air purifier and a TiO₂ photocatalytic filter and found that 83.2% of NO was removed and NO₂ was increased by 12.9% [28].

Most recent studies on TiO₂ have focused on evaluating its air-cleaning performance using cement and stone. In addition, a few studies have quantitatively evaluated the air-cleaning performance of TiO₂ combined with other building materials. TiO₂ photocatalysts have been applied to building materials, pavement materials, and air purifiers

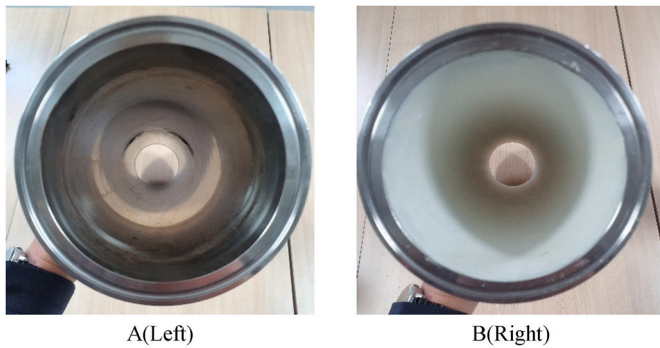


Fig. 4. Condition change test to achieve NO_x reduction. (A) Before applying the coating agent inside the duct and (B) after applying the coating agent inside the duct.

Table 6

Experimental application conditions of ISO 22197-1: 2007.

Classification	Value
UV-A irradiance	10.0 W/m ²
NO gas concentration	1.000 ppm
Temperature	25 ± 2.5 °C
Relative humidity	50%
Number of experiments	3

Table 7

UV-A irradiance applied to the slide-ac at different voltages.

Voltage	UV-A irradiance
90 V	4.0 W/m ²
100 V	6.5 W/m ²
110 V	7.5 W/m ² (25% Down)
125 V	10.0 W/m ² (Basic condition)
135 V	12.5 W/m ² (25% Up)
150 V	15.0 W/m ² (50% Up)

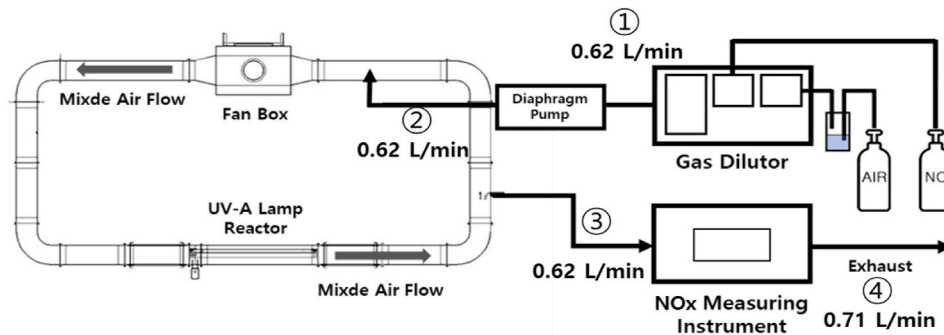


Fig. 5. Flow diagram of the measurement experiment flow.

Table 4

Measurement points and experiment flow values.

Measurement point	Route	Flow rate (Slpm)
①	Dilutor → Pump	0.62
②	Pump → Duct	0.62
③	Duct → NO _x Measuring Instrument	0.62
④	NO _x Measuring Instrument → Exhaust	0.71

Table 5

Details of equipment.





Name	AMI 310, SOM 900		
Measurement	Velocity		
Precision & Limit	Precision	0.1 m/s	
	Limit	25 m/s	
Name	Serinus 40		
Measurement	NO, NO ₂ , NO _x		
Range	0–20 ppm		
Precision	0.4 ppb or 0.5%		
Sample Flow Rate	0.3 Slpm		
Name	DLC-0.5K 220/240		
Capacity	0.5 KVA (500 VA)		
Input/Output	220 V/5–240 V		
(electric) Current	2 A		
Name	Testo 174 H		
Measurement	Temperature, Humidity		
Range	Temperature	–20 ~ +70 °C	
	Humidity	0–100% RH	

Table 8

Experimental NO_x concentration change value.

Classification	NO _x Concentration
75% Down Concentration	0.250 ppm
50% Down Concentration	0.500 ppm
25% Down Concentration	0.750 ppm
Basic Condition Concentration	1.000 ppm

in previous studies. However, there were no cases in which TiO₂ photocatalysts were applied to ventilation ducts. Specifically, as air pollution has become serious, building ventilation systems require the introduction of purified outside air.

Therefore, the main purpose of this study was to purify the polluted outside air introduced into the indoor space through a building ventilation duct system with TiO₂ photocatalyst coatings. A ventilation duct system with TiO₂ photocatalyst coatings was designed and fabricated, and the characteristics of air according to the control of NO_x and UV-A in the ventilation duct system were tested and analyzed in accordance with ISO 22197-1:2007 [29]. The results of this study are expected to be used as basic data for securing the health of occupants in buildings with ventilation systems that introduce polluted outside air.

2. Methods & experiment

2.1. Design and fabrication of the ventilation duct system

The ventilation duct system that was designed and fabricated in this study is illustrated in Fig. 1. Stainless steel, which is resistant to corrosion and does not emit pollutants, was used as for the ventilation duct, and the duct was modularized for easy assembly and disassembly. The

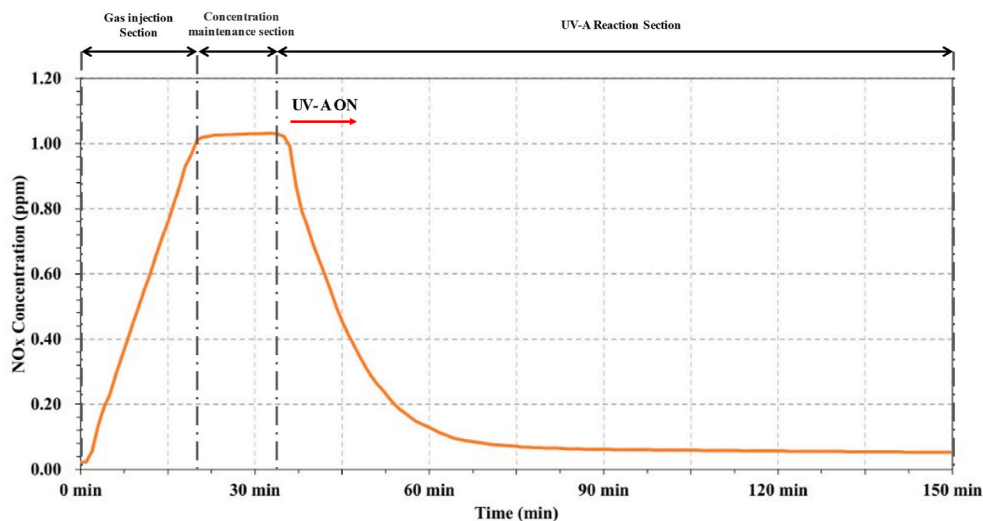


Fig. 6. Conditional application experiment results of ISO 22197-1.

Table 9

Conditional application experiment results of ISO 22197-1.

Classification	Start concentration	End concentration	Concentration difference	Minimum concentration arrival time
NO	1.030 ppm	0.020 ppm	−1.010 ppm (Reduction)	101 min
NO ₂	0.003 ppm	0.033 ppm	+0.030 ppm (Generate)	–
NOx	1.033 ppm	0.053 ppm	−0.980 ppm (Reduction)	101 min

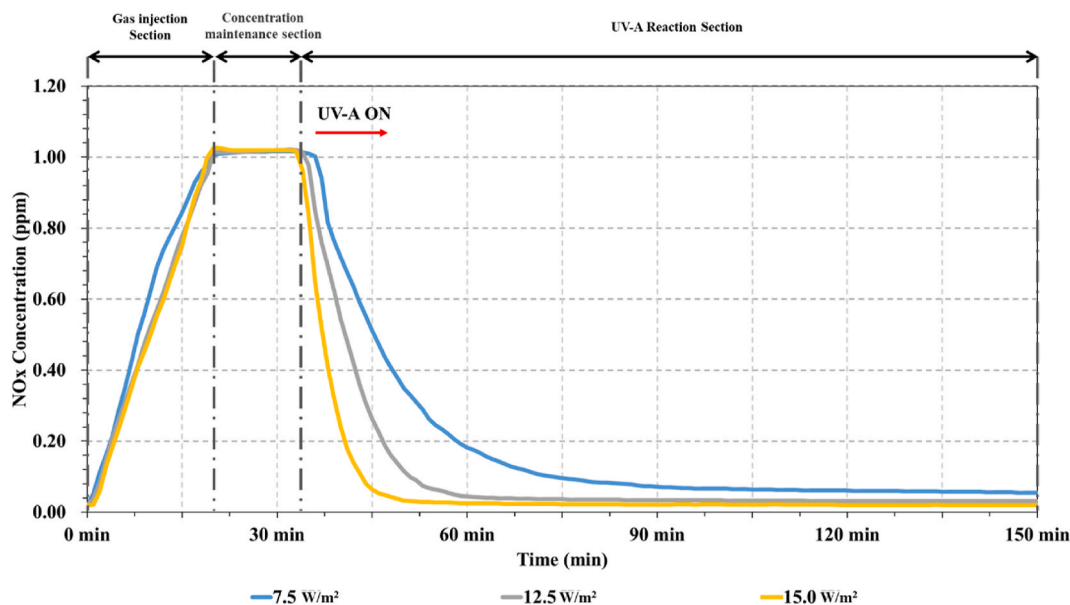


Fig. 7. Experiment results on UV-A variation in irradiance.

module sizes were set to 618 and 309 mm, considering the size of the UV-A lamp. The AC type in Fig. 1 was fabricated using acrylic material, and a thermo-hygrometer was installed in the section to measure the temperature and humidity.

The fan box shown in Fig. 1 was used for the airflow inside the duct. Moreover, a multi-blade fan capable of generating an air volume of up to 300 CMH was installed. The area marked with the red dotted line in Fig. 1 is the section where photochemical reactions between UV-A and the TiO₂ coating agent occur. The coating agent was applied to an area of 0.18 m², which represented approximately 13% of the total area. The amount of the TiO₂ coating agent applied was 30 g. TL-D 18 W BL lamp

(company P), a lamp with a wavelength of 315–400 nm, was used as a UV-A lamp in the experiment. Table 1 presents the distribution of components in the TiO₂ coating used for the ventilation duct system.

2.2. TiO₂ photocatalyst coating agent

The composition ratio of each element of the TiO₂ coating agent used was analyzed using field emission scanning electron microscopy (FESEM) and energy dispersive X-Ray spectroscopy (EDS) mapping. The analysis was conducted by comparing the composition ratio of each element before and after applying the TiO₂ coating agent to the sample

Table 10
Experimental results of UV-A variation with respect to irradiance.

UV-A Irradiance	Start concentration	End concentration	Concentration difference	Minimum concentration arrival time
7.5 W/m ²	1.016 ppm	0.055 ppm	−0.961 ppm	113 min
10.0 W/m ²	1.033 ppm	0.053 ppm	−0.980 ppm	101 min
12.5 W/m ²	1.020 ppm	0.031 ppm	−0.989 ppm	72 min
15.0 W/m ²	1.019 ppm	0.020 ppm	−0.999 ppm	25 min

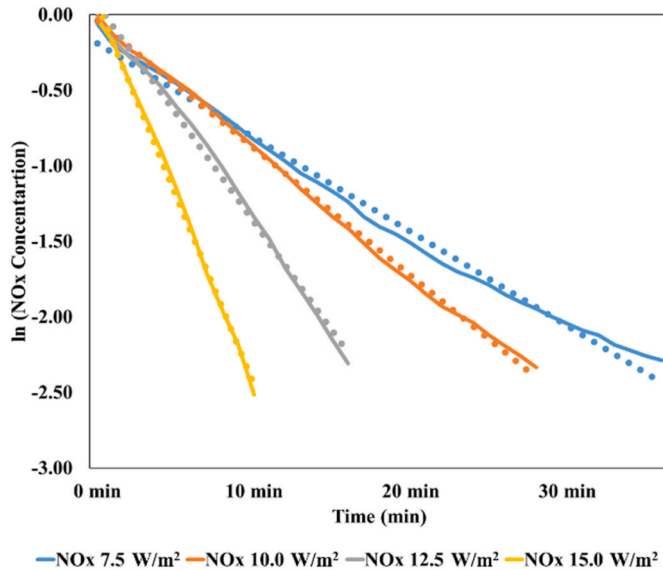


Fig. 8. NOx reduction trend graph with UV-A irradiance.

Table 11
NOx reductions resulting from UV-A irradiance changes.

UV-A Irradiance	Linear exponential function	R ²	Time to reach 90% NOx removal efficiency
7.5 W/m ²	$Y = -0.0623x - 0.1291$	0.9909	37 min (90.28%)
10.0 W/m ²	$Y = -0.0843x + 0.0434$	0.9980	29 min (90.60%)
12.5 W/m ²	$Y = -0.1441x + 0.2101$	0.9936	17 min (90.26%)
15.0 W/m ²	$Y = -0.2513x + 0.3138$	0.9968	11 min (92.06%)

holder (STUB) used for FESEM. Table 2 and Fig. 2 shows the FESEM and EDS mapping equipment [23].

Before the application of the TiO₂ coating agent, the STUB was composed of C (12.84%), O (3.04%), Al (79.34%), and Cu (4.79%), as shown in Table 3 and Fig. 3. Al represented the highest proportion in the STUB. However, after the application of the TiO₂ coating agent, the composition of the STUB was as follows: C (3.47%), O (65.09%), Al (10.39%), and Ti (21.05%), as shown in Table 3 and Fig. 3. Ti, which was not present before the application of the coating agent, was added and the proportion of O significantly increased from 3.04% to 65.09%, confirming the presence of the TiO₂ component in the coating agent used in the experiment.

FESEM and EDS mapping analyses confirmed the NOx removal performance of the TiO₂ coating agent used in the experiment.

For the efficient application of the coating agent on the inside of the fabricated ventilation duct system, the coating agent was applied after the application and hardening of the primer. Fig. 4 shows the inside of the duct before and after the application of the coating agent.

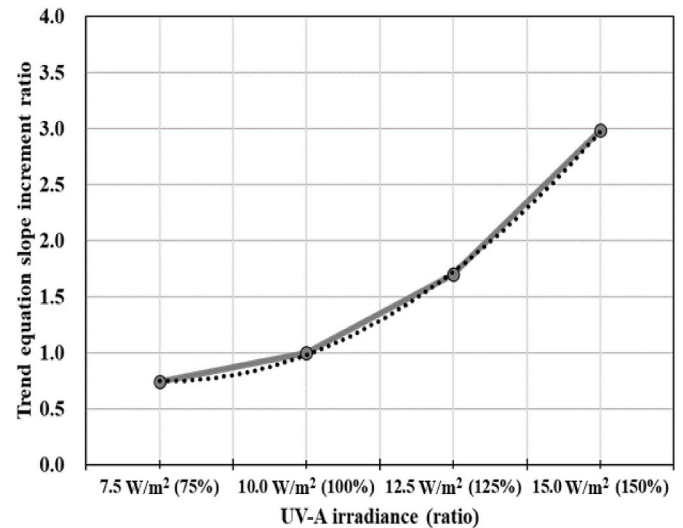


Fig. 9. NOx reduction rate with change in UV-A irradiance.

2.3. Experiment

In the experiment, air conditions were measured according to the control of NOx and UV-A in the ventilation duct system with TiO₂ photocatalyst coatings, as shown in Fig. 5. Table 4 and Fig. 5 show the duct inlet and outlet flow rates, respectively. The flow rate inside the duct was set to 448.66 Slpm during the measurement, and the NOx concentration was confirmed to remain constant.

As shown in Table 4, the flow rate at measurement point ④ is 0.09 Slpm higher than that at measurement points ①, ②, and ③, owing to the inflow of outside air for NOx analysis. Table 5 lists the details of the measurement equipment used in the experiments.

The following three experiments were performed. The experiments were repeated three times, and the average values were used to reduce the errors that may occur in each experiment.

2.3.1. Experiment 1 (Basic condition)

In the basic experiment, NOx (1.000 ppm) and UV-A (10.0 W/m²) were applied to the experiment as default values under the conditions of ISO 22197-1:2007 [29] (see Table 6).

2.3.2. Experiment-2 (UV-A condition change)

The UV-A irradiance control experiment was performed while the UV-A value was varied from 10.0 W/m² (standard) to 7.5 W/m² (25% decrease), 12.5 W/m² (25% increase), and 15.0 W/m² (50% increase) as shown in Table 7. Irradiance was controlled using a voltage controller (slide-ac).

2.3.3. Experiment-3 (NOx concentration change)

Because NOx has a very high concentration level of 1.000 ppm employed in the basic condition and such level does not commonly occur in the atmosphere, the experiment was performed while the concentration was reduced to 75% (0.750 ppm), 50% (0.500 ppm), and 25% (0.250 ppm), which are the concentrations that may occur in the actual environment (refer to Table 8).

3. Results & discussion

3.1. Basic condition result

As shown in Fig. 6, NO gas was injected into the duct for 20 min to reach a NOx concentration of 1.000 ppm, and the concentration was maintained for 10 min in the experiment. The UV-A lamp was then turned on, and the NOx concentration was measured for 120 min.

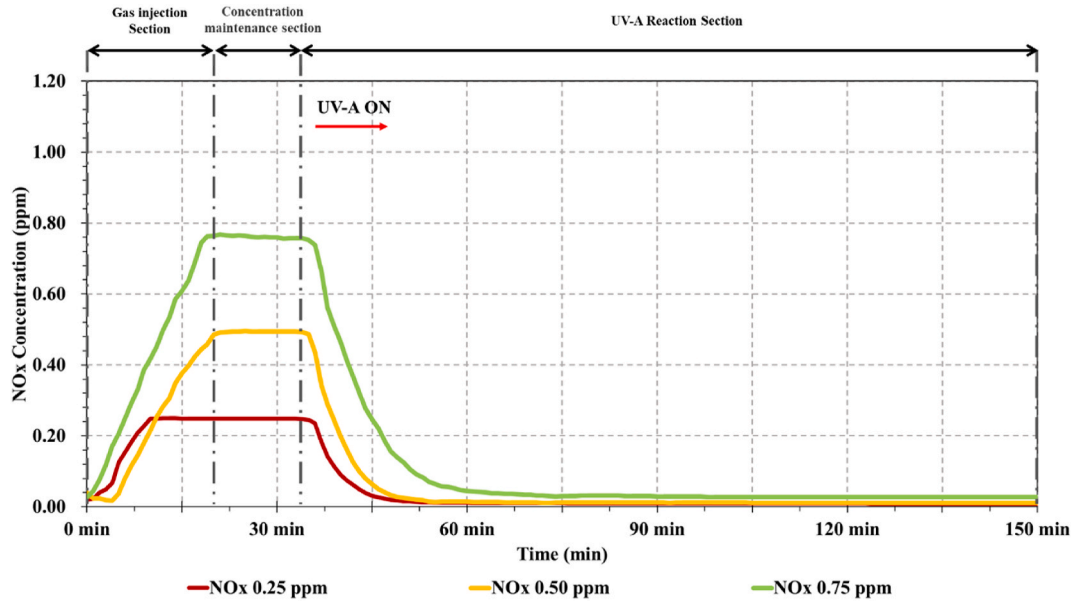


Fig. 10. Experimental results obtained after applying NOx concentration change conditions.

Table 12

Experimental results of applying NOx concentration change conditions.

NOx concentration	Start concentration	End concentration	Concentration difference	Minimum concentration arrival time
0.250 ppm	0.248 ppm	0.008 ppm	-0.240 ppm	66 min
0.500 ppm	0.494 ppm	0.010 ppm	-0.484 ppm	86 min
0.750 ppm	0.756 ppm	0.027 ppm	-0.729 ppm	93 min
1.000 ppm	1.033 ppm	0.053 ppm	-0.980 ppm	101 min

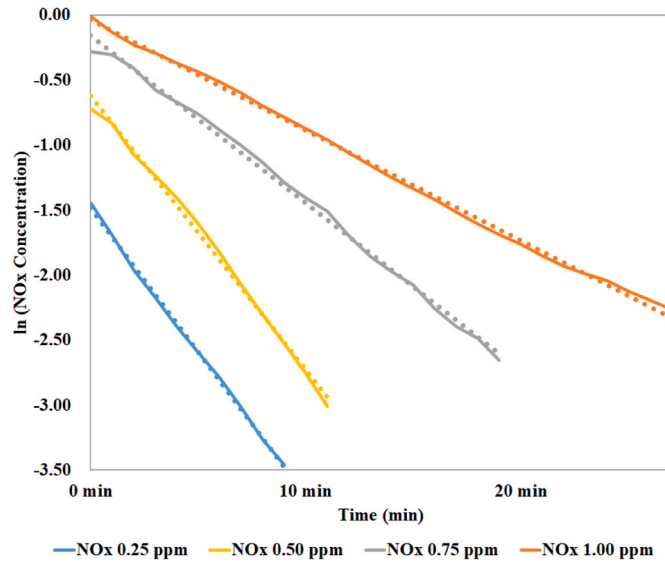


Fig. 11. NOx reduction trend graph with NOx concentration change.

The basic condition results showed that when the NOx concentration was 1.033 ppm and the UV-A irradiance was 10 W/m², the NOx concentration decreased to 0.053 ppm (by 94.87%) for approximately 100 min after turning on the UV-A lamp in the ventilation duct system with TiO₂ photocatalyst coatings, as shown in Table 9.

Table 13

NOx reduction results obtained after NOx concentration change.

NOx concentration	Linear exponential function	R ²	Time to reach 90% NOx removal efficiency
0.250 ppm	$Y = -0.2211x - 1.2647$	0.9987	8 min (90.97%)
0.500 ppm	$Y = -0.2104x - 0.4144$	0.9955	11 min (90.01%)
0.750 ppm	$Y = -0.129x - 0.0267$	0.9963	19 min (90.79%)
1.000 ppm	$Y = -0.0843x + 0.0434$	0.9968	29 min (90.60%)

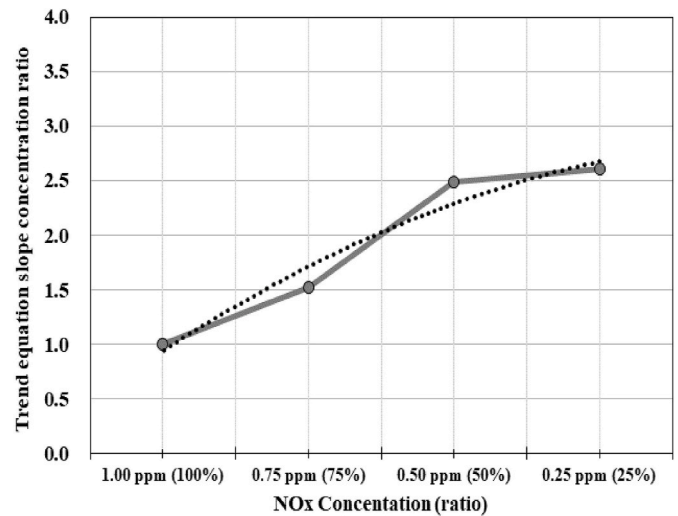


Fig. 12. NOx reduction rate with change in NOx concentration.

3.2. UV-A irradiance control result

Fig. 7 shows the results of the UV-A irradiation control experiment. In the experiment, as in the basic condition, NO_x gas was injected into the duct for 20 min to reach an NO_x concentration of 1.000 ppm, and the concentration was maintained for 10 min. UV-A was then turned on, and the NO_x concentration was measured for 120 min. The measurement was performed according to the UV-A irradiance (7.5, 12.5, and 15.0 W/m²).

Table 10 gives the NO_x concentration reductions observed during operation of the UV-A Lamp and the time required to reach the lowest NO_x concentration. The results of the UV-A irradiance control experiment showed that the NO_x reduction rate at 7.5 W/m² (94.58%) was lower than that under basic conditions (94.87%). When the UV-A irradiance increased to 12.5 and 15.0 W/m², however, the NO_x reduction rate also increased (96.96 and 98.04%, respectively).

Fig. 8 shows the NO_x reduction trend graph based on the UV-A irradiance. As the UV-A irradiance increased, the slope of the trend graph became steeper because of the acceleration of the TiO₂ photocatalytic oxidation reactions. Based on this, the NO_x reduction trend curve according to the UV-A irradiance can be represented by the equations shown in Table 11.

R² was found to be higher than 0.99 for all trend equations according to the UV-A irradiance, indicating a high accuracy. It was confirmed that the trend equation slope representing the reduction rate was proportional to the increase in the UV-A irradiance.

The trend equation slope increment ratio according to UV-A irradiance is shown in Fig. 9. In other words, when the UV-A irradiance increased from 10.0 to 12.5 and 15.0 W/m², the trend equation slope increased by approximately 1.7 and 2.98 times, respectively, confirming that the pollutant concentration reduction effect increased alongside the increase in UV-A irradiance.

3.3. NO_x concentration control result

The NO_x concentration of 1.000 ppm, which was applied to the basic condition, was too high to represent the general environment. Therefore, measurements were performed the reduced NO_x concentration at 75% (0.750 ppm), 50% (0.500 ppm), and 25% (0.250 ppm) compared to 1.000 ppm.

As shown in Fig. 10, when the results of reactions with UV-A 10 W/m² were measured while the NO_x concentration was reduced from 1.000 ppm to 0.750, 0.500, and 0.250 ppm, the time required to reach the minimum concentration was the shortest (66 min) at a NO_x concentration of 0.250 ppm. This indicates that the time required to remove NO_x through reactions with TiO₂ photocatalysts increases as the NO_x concentration in the air inside the duct increases (refer to Table 12).

Fig. 11 shows the slope of the trend equation according to the NO_x concentration. As the NO_x concentration decreased from 1.000 to 0.250 ppm, the time required to reach 90% NO_x removal efficiency decreased from 29 to 8 min. In other words, it was confirmed that the NO_x removal rate increased as the NO_x concentration decreased in the ventilation duct with photocatalyst coatings. This NO_x reduction trend can be represented by trend equations, as shown in Table 13. R² was found to be higher than 0.99 for the trend equations.

Fig. 12 shows the trend equation of the slope concentration ratio according to the NO_x concentration. When the NO_x concentration was reduced from 1.000 to 0.750, 0.500, and 0.250 ppm, the pollutant concentration reduction rate increased by approximately 1.5, 2.48, and 2.61 times, respectively.

The above results confirmed that the pollutant removal efficiency in the ventilation duct with photocatalyst coatings increased as the UV-A irradiance increased beyond 10 W/m², and the NO_x concentration became lower than 1.000 ppm.

4. Conclusion

This study analyzed the characteristics of air through a ventilation duct system with TiO₂ photocatalyst coatings when polluted outside air is introduced into the indoor space using a building ventilation system. To this end, a ventilation duct system with TiO₂ photocatalyst coatings was designed and fabricated, and the characteristics of air were analyzed according to the control of the UV-A irradiance and NO_x concentration. The results of this study can be summarized as follows.

First, many previous studies have been conducted on the application of TiO₂ photocatalysts to building materials, pavement materials, and air purifiers, but there have been no studies on their application to building ventilation ducts. Therefore, in this study, an air purification experiment was performed by applying TiO₂ photocatalysts to the ventilation duct.

Second, the air conditions were measured according to the control of NO_x and UV-A irradiance in the ventilation duct system with TiO₂ photocatalyst coatings. When the basic conditions of NO_x (1.000 ppm) and UV-A at 10.0 W/m², given in ISO 22197-1:2007, were applied, the NO_x concentration decreased to 0.053 ppm (by 94.87%) at approximately 100 min after turning on the UV-A lamp. This confirmed that the NO_x concentration decreased when the air that passed through the photocatalyst-coated duct reacted with the UV lamp. In addition, according to the UV-A irradiance and NO_x concentration during the experiments, we confirmed that the pollutant removal efficiency increased as the UV-A irradiance increased beyond 10 W/m² and the NO_x concentration became lower than 1.000 ppm. When these results were verified through trend equations, the R² value was found to be higher than 0.99.

Third, the experimental results of this study confirmed that it is possible to reduce PM precursors through ventilation duct systems with photocatalyst coatings, even in the general atmospheric environment. This presents the possibility of using ventilation duct systems with photocatalyst coatings as measures to reduce PM precursors.

However, in this study, the circulation method was used when the experiment was performed using a ventilation duct system with photocatalyst coatings. Therefore, it is necessary to evaluate the PM precursor reduction performance through a combination of outside air introduction and the circulation method.

The experimental results of this study are expected to serve as basic data for evaluating the performance of building ventilation systems with TiO₂ photocatalysts.

Funding

This work was supported by the Korea Agency for Infrastructure Technology Advancement (KAITA) grant funded by the Ministry of Land, Infrastructure, and Transport, South Korea (grant number 21SCIP-B146254-04) and Chung-Ang University Research Scholarship Grant in 2021, South Korea.

Declaration of competing interest

The authors declare that they have no known competing financial interests or personal relationships that could have appeared to influence the work reported in this paper.

References

- [1] IQAir, World air quality report (region & city PM_{2.5} ranking), Available online: <https://www.iqair.com/world-most-polluted-cities/world-air-quality-report-2019-en.pdf>, 2019.
- [2] M.R. Cho, Problems and Countermeasures of High Concentration Particulate Matter, vol. 2, The Korea Transport Institute, Monthly KOIT Magazine on Transport, 2018, pp. 2–4.
- [3] Comprehensive Plan for Particulate Matter Management, the Department of the Environment, 2019, pp. 1–4.

- [4] M.U. Ali, G. Liu, B. Yousaf, H. Ullah, Q. Abbas, M.A.M. Munir, A systematic review on global pollution status of particulate matter-associated potential toxic elements and health perspectives in urban environment, *Environ. Geochem. Health* 41 (3) (2019) 1131–1162, <https://doi.org/10.1007/s10653-018-0203-z>.
- [5] WHO Europe, Health Effects of Particulate Matter, Available online: https://www.euro.who.int/_data/assets/pdf_file/0006/189051/Health-effects-of-particulate-matter-final-Eng.pdf.
- [6] Manual for Indoor Air Quality Management of Daycare Centers and Children's Welfare Facilities, the Department of the Environment, 2011, p. 10. Available online: http://www.jgicare.or.kr/bbs/board.php?bo_table=document&wr_id=86&sca=%EB%AC%B8%EC%84%9C%EC%9E%90%EB%A3%8C%EC%8B%A4.
- [7] J.S. Park, Amount of Particulate Matter Inflow by Ventilation System, vol. 12, Korea Institute of Architectural Sustainable Environment and Building Systems, 2018, pp. 28–32, 2.
- [8] J.M. Back, The Size-Resolved Impact of Outdoor Particulate Matter on Indoors, Graduate Master's Degree in Engineering, Seoul National University, 2015.
- [9] G. Cao, Effect of ventilation on indoor airborne microbial pollution control, in: 2008 International Conference on Biomedical Engineering and Informatics, 2008, pp. 27–30, <https://doi.org/10.1109/BMEI.2008.112>.
- [10] Y.P. Kim, Air pollution in Seoul caused by aerosols, *J. Korean Soc. Atmos. Environ.* 22 (5) (2006) 535–553.
- [11] Z. Wang, J. Liu, Springtime PM_{2.5} elemental analysis and polycyclic aromatic hydrocarbons measurement in high-rise residential buildings in Chongqing and Xian, China, *Energy, Build* 173 (2018) 623–633, <https://doi.org/10.1016/j.enbuild.2018.06.003>.
- [12] M.M. Ballari, M. Hunger, G. Hüskens, H.J.H. Brouwers, NO_x photocatalytic degradation employing concrete pavement containing titanium dioxide, *Appl. Catal., B* 95 (2010) 245–254, <https://doi.org/10.1016/j.apcatb.2010.01.002>.
- [13] A. Fujishima, X. Zhang, D.A. Tryk, TiO₂ photocatalysis and related surface phenomena, *Surf. Sci. Rep.* 63 (2008) 515–582, <https://doi.org/10.1016/j.surfrep.2008.10.001>.
- [14] R. Wang, M. Shi, F. Xu, Y. Qiu, P. Zhang, K. Shen, Q. Zhao, J. Yu, Graphdiyne-modified TiO₂ nanofibers with osteoinductive and enhanced photocatalytic antibacterial activities to prevent implant infection, *Nat. Commun.* 11 (2020) 4465, <https://doi.org/10.1038/s41467-020-18267-1>.
- [15] L. Cassar, C. Pepe, G. Tognon, G.L. Guerrini, R. Amadelli, White cement for architectural concrete, possessing photocatalytic properties, in: *Proceedings of the 11th International Congress on the Chemistry of Cement*, Durban, South Africa, 2003.
- [16] S. Shen, M. Burton, B. Jobson, L. Haselbach, Pervious concrete with titanium dioxide as a photocatalyst compound for a greener urban road environment, *Construct. Build. Mater.* 35 (2012) 874–883, <https://doi.org/10.1016/j.conbuildmat.2012.04.097>.
- [17] C. Cárdenas, J.I. Tobón, C. García, J. Vila, Functionalized building materials: photocatalytic abatement of NO_x by cement pastes blended with TiO₂ nanoparticles, *Construct. Build. Mater.* 36 (2012) 820–825, <https://doi.org/10.1016/j.conbuildmat.2012.06.017>.
- [18] A.M. Ramirez, K. Demeestere, N. De Belie, T. Mäntylä, E. Levänen, Titanium dioxide coated cementitious materials for air purifying purposes: preparation, characterization and toluene removal potential, *Build. Environ.* 45 (2010) 832–838, <https://doi.org/10.1016/j.buildenv.2009.09.003>.
- [19] H. Wang, K. Jin, X. Dong, S. Zhan, C. Liu, Preparation technique and properties of nano-TiO₂ photocatalytic coatings for asphalt pavement, *Appl. Sci.* 8 (11) (2018) 2049, <https://doi.org/10.3390/app8112049>.
- [20] D. Wang, Z. Leng, M. Hüben, M. Oeser, B. Steinauer, Photocatalytic pavements with epoxy-bonded TiO₂-containing spreading material, *Construct. Build. Mater.* 107 (2016) 44–51, <https://doi.org/10.1016/j.conbuildmat.2015.12.164>.
- [21] M. Luna, M.J. Mosquera, H. Vidal, J.M. Gatica, Au-TiO₂/SiO₂ photocatalysts for building materials: self-cleaning and de-polluting performance, *Build. Environ.* 164 (2019) 106347, <https://doi.org/10.1016/j.buildenv.2019.106347>.
- [22] M. Lettieri, D. Colangiuli, M. Masieri, A. Calia, Field performances of nanosized TiO₂ coated limestone for a self-cleaning building surface in an urban environment, *Build. Environ.* 147 (2018) 506–516, <https://doi.org/10.1016/j.buildenv.2018.10.037>.
- [23] Y.W. Song, M.Y. Kim, M.H. Chung, Y.K. Yang, J.C. Park, NO_x-reduction performance test for TiO₂ paint, *Molecules* 45 (2020) 4087, <https://doi.org/10.3390/molecules25184087>.
- [24] Y.K. Zhao, T.T. Tsai, H.J. Wang, H.T. Chiu, Research on bacteriostasis for nanoscale Ag/TiO₂-HVAC system, *Adv. Sci. Lett.* 4 (4–5) (2010) 1828–1832, <https://doi.org/10.1166/asl.2011.1346>.
- [25] T.S. Le, T.H. Dao, D.C. Nguyen, H.C. Nguyen, I.L. Balikhin, Air purification equipment combining a filter coated by silver nanoparticles with a nano-TiO₂ photocatalyst for use in hospitals, *ANSN* 6 (1) (2015), 015016, <https://doi.org/10.1088/2043-6262/6/1/015016>.
- [26] M. Kim, H. Jung, E. Park, J. Jung, Performance of an air purifier using a MnO_x/TiO₂ catalyst-coated filter for the decomposition of aldehydes, VOCs and ozone: an experimental study in an actual smoking room, *Build. Environ.* 186 (2020) 107247, <https://doi.org/10.1016/j.buildenv.2020.107247>.
- [27] K.P. Yu, G.W.M. Lee, W.M. Huang, C.C. Wu, C.L. Lou, S. Yang, Effectiveness of photocatalytic filter for removing volatile organic compounds in the heating, ventilation, and air conditioning system, *J. Air Waste Manag. Assoc.* 56 (5) (2006) 666–674, <https://doi.org/10.1080/10473289.2006.10464482>.
- [28] C.H. Ao, S.C. Lee, Indoor air purification by photocatalyst TiO₂ immobilized on an activated carbon filter installed in an air cleaner, *Chem. Eng. Sci.* 60 (1) (2005) 103–109, <https://doi.org/10.1016/j.ces.2004.01.073>.
- [29] DIN German Institute for Standardization, Fine Ceramics (Advanced Ceramics, Advanced Technical Ceramics)—Test Method for Air-Purification Performance of Semiconducting Photocatalytic Materials—Part 1: Removal of Nitric Oxide, Beuth Verlag GmbH, Berlin Germany, 2007.